Journal of Alzheimer's Disease 53 (2016) 1161–1172
DOI 10.3233/JAD-151137
IOS Press

Adults at Increased Alzheimer's Disease Risk Display Cognitive-Motor Integration Impairment Associated with Changes in Resting-State Functional Connectivity: A Preliminary Study

Kara M. Hawkins[1] and Lauren E. Sergio*
School of Kinesiology and Health Science, Centre for Vision Research, York University, Toronto, ON, Canada

Handling Associate Editor: Manuel Montero-Odasso

Accepted 2 May 2016

Abstract.
Background: Many neuroimaging parameters have demonstrated utility as biomarkers in preclinical AD, including resting-state functional connectivity in the default mode network. However, neuroimaging is not a practical, cost effective screening instrument.
Objective: Here we investigate the relationship between performance on a cognitive-motor integration assessment and alterations in resting-state functional connectivity in an at-risk population.
Methods: Three groups of ten adults (young: mean age = 26.6 ± 2.7, low AD risk: mean age = 58.7 ± 5.6, and high AD risk: mean age = 58.5 ± 6.9) performed a simple cognitive-motor integration task using a dual-touchscreen laptop and also underwent functional magnetic resonance imaging at rest.
Results: We found poorer cognitive-motor integration performance in high AD risk participants, as well as an association with lower resting-state functional connectivity in this group.
Conclusion: These findings provide novel insight into underlying AD-related brain alterations associated with a behavioral assessment that can be easily administered clinically.

Keywords: Aging, ApoE4, dementia, functional magnetic resonance imaging, geriatric assessment, population at risk, psychomotor performance

INTRODUCTION

Current clinical criteria for the probable diagnosis of Alzheimer's disease (AD), largely involving behavioral assessments of short-term and episodic memory, can only identify individuals after significant damage to the brain has already occurred [1]. In order to develop and evaluate treatments to prevent or delay neurodegeneration, research investigating early disease detection strategies is essential. In recent years, four approaches in particular have been widely used to identify individuals at increased risk for AD [1]: 1) apolipoprotein E epsilon 4 (ApoE4) genotyping, in which individuals who carry the ApoE4 allele

[1]Present address: Toronto Rehabilitation Institute, University Health Network, Toronto, ON, Canada.

*Correspondence to: Lauren E. Sergio, Ph.D., York University, School of Kinesiology and Health Science, 4700 Keele Street, Toronto, ON M3J 1P3, Canada. Tel.: +1 416 736 2100/Ext. 33641; Fax: +1 416 736 5774; E-mail: lsergio@yorku.ca.

are at greater risk of late-onset AD, amyloid deposits in the walls of cerebral blood vessels, and cognitive decline in normal aging [2], 2) family history, in which individuals who have a first-degree relative with AD are more likely to develop the disease then those who do not [3–5], 3) amyloid-beta (Aβ) imaging, whereby a high level Aβ deposition in the brains of cognitively healthy individuals is associated with increased AD risk and future declines in episodic and working memory [6], and 4) neuropsychological tests of subtle cognitive changes (i.e., mild cognitive impairment, MCI), whereby a clinical diagnosis of MCI (particularly amnestic MCI) is associated with increased risk of progressing to AD dementia [7]. Using these methods to identify at-risk groups and compare neuroimaging measures relative to cognitively healthy low-risk groups can provide important insight into early brain changes, which may prove useful in developing biomarkers for the early detection of AD pathology and the prediction of dementia before the onset of clinical symptoms.

The accumulation of recent evidence from functional connectivity and DTI studies provides support for the view that AD is a disconnection syndrome, with cognitive impairment resulting from disruption to functional activity across interconnected brain regions [8, 9]. Furthermore, evidence in preclinical populations of functional and structural disconnection suggests that this may be an early identifying feature of the disease [10–22]. For example, several studies using resting-state functional magnetic resonance imaging (rs-fMRI) in preclinical AD have demonstrated reduced functional connectivity across interconnected cortical regions including the precuneus, lateral parietal, lateral temporal, and medial prefrontal cortices, known as the default mode network (DMN), that are normally active in correlation with each other during rest [11–15]. One way to test the integrity of communication among different brain regions is to employ a task that requires the integration of different domains. To this end, there have been recent behavioral demonstrations of impaired visuomotor control under cognitively demanding conditions, which requires sound connections between disparate brain regions, in early and preclinical AD [23–31]. Specifically, these populations demonstrate impaired reaching performance on visually-guided tasks that rely on the ability to inhibit the default tendency to move towards a visual stimulus, in order to move in the opposite direction and/or in a different spatial plane [20–24]. Initial evidence for the neural underpinnings of such impairment comes from our previous structural neuroimaging work in preclinical AD, which demonstrated an association between diffusion tensor imaging (DTI) measures of white matter (WM) integrity and cognitive-motor performance [32].

Here we test the utility of a simple behavioral cognitive-motor integration task to serve as a marker for disrupted reciprocal communication in resting-state functional neural networks. Specifically, we test the hypothesis that the cognitive-motor integration deficits observed in high AD risk participants may be associated with brain alterations disrupting reciprocal communication in the DMN. By investigating the relationship between measures of neural network efficiency and simple kinematic measures of cognitive-motor integration performance in preclinical AD, we provide novel insight into a pragmatic, clinically accessible behavioral assessment for early disease detection.

MATERIALS AND METHODS

Subjects

The same thirty right-handed female participants as in Hawkins et al. [32] were included in this study: 10 healthy young controls (mean age = 26.6 ± 2.7), 10 low AD risk older adults (mean age = 58.7 ± 5.6), and 10 high AD risk older adults (mean age = 58.5 ± 6.9). In this preliminary study, we focused on female participants due to the greater prevalence of AD in this population [33, 34], evidence that women who carry the ApoE4 allele may be particularly vulnerable to AD pathology affecting brain connectivity [35], and in order to avoid sex-related confounds inherent in brain imaging studies when there is not enough data available to perform sex-difference analyses. Exclusion criteria were vision or upper-limb impairments, medical conditions that would hinder task performance (e.g., severe arthritis), neurological or psychiatric illnesses (e.g., schizophrenia, depression, alcoholism, epilepsy, Parkinson's disease), and/or history of stroke or severe head injury. Participants were not specifically questioned about chronic conditions such as hypertension or diabetes, which could have an impact on white matter integrity and brain connectivity, however none reported these conditions during the screening interview and there is no reason to suspect any group differences. Classification as high AD risk was based on reporting either a maternal, multiple, or early-onset family history of AD [3–5], but with no cognitive impairment

as indicated by the Montreal Cognitive Assessment (MoCA). Since paternal history alone may not carry the same increased risk as maternal history, this was not included as part of the high AD risk classification [36–38]. Low AD risk participants were age-matched with high AD risk participants and reported no dementia of any type within their known family history, expressed no memory complaints beyond normal expectations for their age and scored at or above age- and education-adjusted norms on the MoCA. Older adult participants also provided saliva samples for ApoE genotyping (Viaguard Accumetrics,Toronto ON), which supported the increased genetic risk in our positive family history sample (i.e., 80% ApoE4 carriers). Demographic characteristics for all study participants are summarized in Table 1. The study protocol was approved by the Human Participants Review Sub-Committee, York University's Ethics Review Board, and conforms to the standards of the Canadian Tri-Council Research Ethics guidelines.

Rule-based visuomotor assessment

Our visuomotor assessment is described in detail in Hawkins and Sergio [26]. Briefly, participants were tested on two visuomotor transformation tasks presented on an Acer Iconia 6120 dual-touchcreen tablet. In one task the spatial location of the viewed target and the required movement were the same (standard task), and in the other, more cognitively demanding non-standard task, the location of the viewed target was dissociated from the required movement (i.e., in both a different spatial plane and in the opposite direction; Fig. 1A). These two tasks were presented in a random order across participants and consisted of five pseudo-randomly presented trials to each of four peripheral targets (from a common central 'home' target), for a total of 20 trials per condition and 40 trials per participant (Fig. 1B). Participants were instructed to move as quickly and accurately as possible. Each participant was also given two practice trials per target prior to each condition and their eyes were monitored throughout the experiment using a webcam to ensure compliance with the task instructions (i.e., always look toward the visual target).

Imaging data acquisition

A 3 Tesla Siemens Tim Trio scanner was used to acquire anatomical and functional magnetic resonance imaging (MRI) data. Sequences included a high-resolution T1-weighted anatomical scan using magnetization prepared rapid gradient echo (MPRAGE), and an echo planar imaging (EPI) sequence sensitive to blood-oxygenation-level dependent (BOLD) contrast. The MPRAGE sequence consisted of 192 sagittal slices with a slice thickness of 1 mm with no gap, field of view (FOV) of 256 mm × 256 mm, and a matrix size of 240 × 256, resulting in a voxel resolution of $1 \times 1 \times 1\ mm^3$ [repetition time (TR) = 2300 ms, echo time (TE) = 2.96 ms, flip angle = 9°]. For the functional sequence, participants were asked to lie still in the scanner with their eyes closed for six minutes and to let their mind wander. 35 axial slices were acquired with a TR of 2000 ms, TE of 30 ms, flip angle of 90°, slice thickness of 4 mm with no gap, FOV of 210 mm × 210 mm, and matrix size of 56 × 70, resulting in a voxel resolution of $3 \times 3 \times 4\ mm^3$.

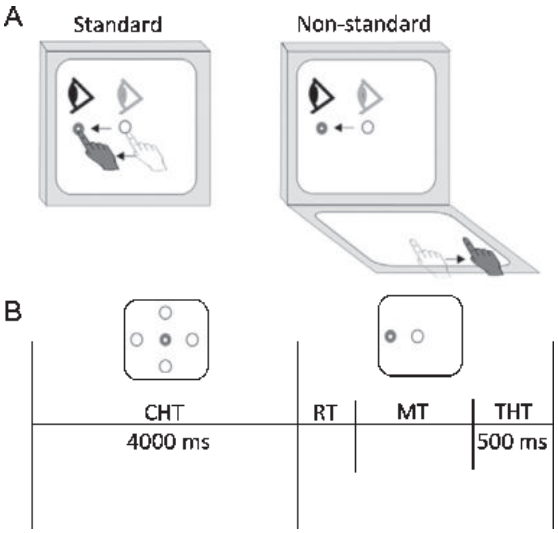

Fig. 1. A) Schematic drawing of the two experimental conditions. Light grey circle, eye, and hand symbols denote the starting position for each trial (i.e., the home target). Dark grey eye and hand symbols denote the instructed eye and hand movements for each task. Dark grey circle denotes the peripheral target, presented randomly in one of four locations. White square denotes the cursor feedback provided during each condition. B) Trial timing. Open circles denote non- illuminated target locations. Disappearance of the home target (which occurred at the same time as presentation of the peripheral target) served as the "go-signal" to initiate movement. CHT, center hold time; RT, reaction time; MT, movement time; THT, target hold time. Reprinted with permission from Hawkins et al. [32].

Kinematic data analysis

A custom written C++ application was used to record and convert the touchscreen data to MATLAB

Table 1
Demographic characteristics of subjects

	Young	Low AD Risk	High AD Risk
Number	10	10	10
Age (SD)	26.6 (2.7)	58.7 (5.6)	58.5 (6.9)
Years of education (SD)	–	17.9 (3.1)	16.8 (3.1)
MoCA score (SD)	–	27.9 (1.7)	28.3 (2.2)
ApoE genotype (% E4 carriers)	–	20%	80%

SD, standard deviation; MoCA, Montreal Cognitive Assessment; ApoE, apolipoprotein E.

format in order to calculate kinematic outcome measures [26]. On- and off-axis constant errors (CE), measuring accuracy, were computed as the average distance between the target and the ballistic (initial) movement endpoints. Variable error (VE), measuring precision, was computed as the standard deviation of the ballistic movement endpoints. Corrective movements (CPL: corrective path length) were quantified as the difference between the total path length and the ballistic path length. Reaction time (RT) and movement time (MT) were calculated as the time between disappearance of the home target ('go signal') and movement onset, and the time between movement onset and the final movement endpoint, respectively. All kinematic measures were averaged across the four peripheral targets. For the non-standard condition, these kinematic measures were summarized into error and timing scores by calculating z-scores and averaging across the CE, VE, and CPL variables, and the RT and MT variables, respectively. These performance error and timing scores from the non-standard condition were then used to assess the relationship between cognitive-motor performance and resting-state functional connectivity in our seed-based correlational analyses.

Imaging data analysis

Imaging data were analyzed using the Oxford Centre for Functional Magnetic Resonance Imaging of the Brain (FMRIB) Software Library (FSL - http://www.fmrib.ox.ac.uk/fsl; [39]). First, in order to identify regions with coherent spontaneous fluctuations in the BOLD signal, a temporally concatenated independent component analysis (ICA) was applied to the resting state data using FSL's MELODIC. For each experimental group, the 2D matrices of each subject's preprocessed (i.e., high-pass filtered at 0.01 Hz, MCFLIRT motion corrected, slice timing corrected, spatially smoothed by an 8 mm FWHM Gaussian kernel, and registered to standard MNI space) functional data set were stacked on top of each other, and then a single ICA was run on this concatenated data matrix. This approach allowed us to look for common spatial patterns in the resting state data without assuming that the associated temporal response was consistent between subjects. In order to minimize false-positives, a threshold level of 0.66 was used. The spatial maps generated by the MELODIC ICA allowed us to identify the component representing the DMN, which was then isolated using the 'fslsplit' command. In order to estimate a "version" of the healthy young group-level DMN functional connectivity for each subject, the FSL 'dual_regression' command was used to regress the young DMN spatial map into each subject's 4D dataset, resulting in a set of time courses. These time courses were then regressed into the same 4D dataset to get subject-specific spatial maps of the DMN [40]. The FSL 'cluster' and 'fslmaths' commands were also used on the subject-specific spatial maps in order to determine the peak activations (local maxima) and cluster sizes within each subject's DMN.

In order to conduct seed-based analyses, the DMN cluster coordinates generated in standard MNI space by FSL MELODIC for each subject were converted to functional space using the FSL command 'std2imgcoord'. Eight seed regions were isolated, including the precuneus (PCUN), medial frontal cortex, right/left parietal cortex, right/left middle temporal gyrus (MTG), and right/left middle frontal gyrus (MFG). Seed masks (6 mm radius) for each subject were then generated around these coordinates in functional space. Next, the raw functional data were preprocessed, which included applying a high pass filter (0.01 Hz), motion correction (MCFLIRT; [41]), slice timing correction (interleaved), removal of non-brain structures, spatial smoothing (6 mm FWHM), and registration to both brain-extracted anatomical (BET; [42]) and standard (MNI152) images. A 5th order bandpass Butterworth filter was then applied in MATLAB in order to include only low-frequency fluctuations in the BOLD signal between 0.01 and 0.1 Hz [43]. These preprocessed

and filtered resting state data were then used to calculate the average time series of all voxels in each seed mask for each volume in every subject. In order to calculate mean white matter, cerebral spinal fluid, and global signals for use, along with the translational and rotational motion correction parameters, as nuisance regressors, the brain-extracted anatomical images were also segmented using FMRIB's Automated Segmentation Tool (FAST; [44]). Prior to running group-level statistical analyses, within subject first-level analyses were run for each seed region using FSL's FMRI Expert Analysis Tool (FEAT), with the above nuisance regressors entered as additional confound variables and the seed time course entered as the predictor variable.

Statistical analysis

Statistical analyses of the behavioral data were carried out in SPSS and included a mixed-design analysis of variance (ANOVA) to compare all six kinematic measures across the two task conditions and between the three experimental groups, as well as one-way ANOVAs to compare the summarized non-standard error and timing *z*-scores between the three experimental groups. *Post hoc* analyses were adjusted for multiple comparisons using Bonferroni correction and were considered statistically significant at $p < 0.05$.

In order to statistically compare the DMN spatial maps between groups, permutation testing (thresholded at $p < 0.05$ and corrected for multiple comparisons using threshold-free cluster enhancement - TFCE) was applied using the FSL 'randomise' command. Peak activations and cluster sizes for the six classic DMN clusters (precuneus, medial frontal, right/left parietal, and right/left temporal; [8, 45]) were also compared between the high and low AD risk older adult groups using independent samples t-tests in SPSS (alpha-level = 0.05).

Since no significant age-related declines in DMN functional connectivity were observed (based on the DMN spatial maps permutation testing between young and older adult low AD risk groups), we restricted our seed-based correlational analyses examining the relationship between resting-state functional connectivity and cognitive-motor performance to older adult participants. Specifically, group-level analyses comparing low and high AD risk older adults, with error and timing scores entered as covariates of interest, were run separately in FEAT for each DMN seed region using FMRIB's Local Analysis of Mixed Effects modeling (FLAME 1; cluster-thresholding for multiple comparisons: $z = 2.7$, $p = 0.05$). The purpose of this analysis was to examine the effects of error and timing scores on functional connectivity between the eight isolated DMN seed regions and the rest of the brain. Specifically, a significant positive effect of error or timing score would suggest an association between greater functional connectivity and poorer performance, whereas a significant negative effect would suggest the expected association between impaired functional connectivity and poorer performance (i.e., larger error and timing scores). For seed regions where significant effects of error and/or timing score(s) on functional connectivity were found, mean z-transformed *r*-values across all voxels were calculated for each participant and scatterplots were generated by correlating these values with error or timing scores in SPSS (two-tailed Pearson's *r;* alpha-level = 0.05).

RESULTS

Kinematic data

The ANOVA analyses demonstrated that all three groups performed similarly across all outcome measures in the standard visuomotor task, whereas performance in the non-standard task was significantly slower, less accurate and less consistent in the high AD risk group. These cognitive-motor deficits observed in high AD risk participants are summarized in Fig. 2, illustrating that error scores were significantly larger in high AD risk relative to both young and low AD risk participants ($F_{2,27} = 21.39$, $p < 0.0001$; *post-hoc*: high AD risk - young = 4.95, $p < 0.00001$, high AD risk - low AD risk = 4.04, $p < 0.0001$), and timing scores were significantly longer in high AD risk relative to young participants ($F_{2,27} = 5.31$, $p = 0.011$; *post-hoc*: high AD risk - young = 1.87, $p = 0.009$).

Imaging data

Significant mean co-activations with the young group-level DMN component for both the low (red-yellow) and high (blue-light blue) AD risk older adult groups are displayed in Fig. 3A ($p < 0.02$, corrected). Figure 3B quantifies the sizes and peak activations of these DMN clusters, revealing a tendency towards smaller cluster sizes and lower peak activations in the high AD risk group. Statistical comparisons between

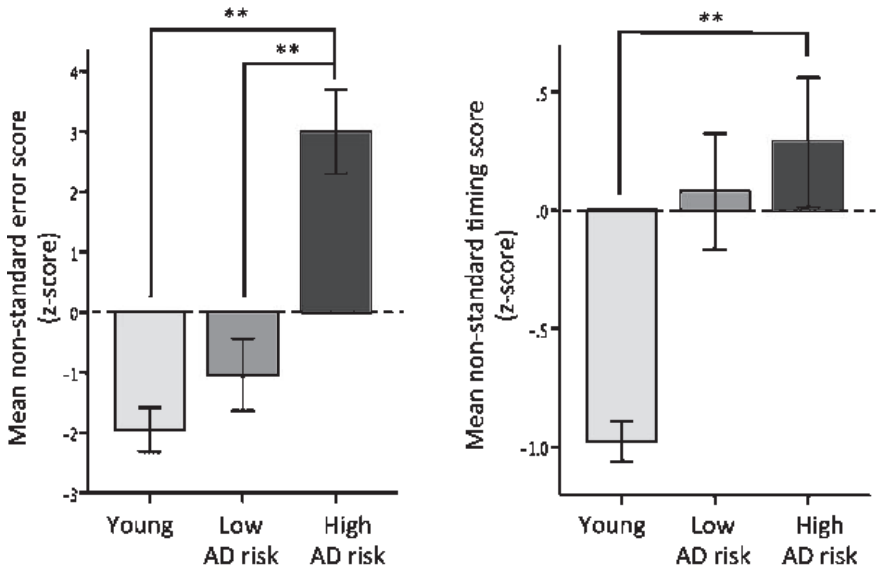

Fig. 2. Mean z-scores for error and timing kinematic measures in the non-standard task across groups (young: light grey bars, low AD risk: medium grey bars, high AD risk: dark grey bars). Note that higher error scores reflect less accuracy and precision and higher timing scores reflect longer reaction and movement times. Means ± 1 SEM, $^{**}p \leq 0.01$. Reprinted with permission from Hawkins et al. [32].

groups revealed that peak activation within the right parietal cluster was significantly lower in the high AD risk group ($t_{18} = 2.59, p = 0.019$). Figure 3C illustrates the permutation test results, revealing regions of significantly greater DMN functional connectivity in low AD risk relative to high AD risk participants ($p < 0.02$, corrected). These regions include the precuneus/posterior cingulate, anterior cingulate, superior frontal gyrus (SFG), MFG, left post- and pre-central gyri, and the right thalamus. Coordinates in standard space (MNI152), Harvard-Oxford structural labels, and significance values for these clusters are listed in Table 2. There were no regions of significantly greater DMN functional connectivity in the high AD risk group relative to the low AD risk group, as well as no significant age-related declines in DMN functional connectivity in the low AD risk older adult group relative to the young adult group.

In support of our hypothesis, significant correlations were found between cognitive-motor performance and resting-state functional connectivity in older adult participants. Specifically, we found that larger error scores were associated with lower functional connectivity between the left MFG and right posterior parietal regions (Fig. 4A), as well as between the right MTG and the right thalamus/basal ganglia (Fig. 4B). We also found that slower timing scores were associated with lower functional connectivity between the right PCUN and left frontal regions (Fig. 4C), as well as between the right MFG and left frontal regions (Fig. 4D). These significant effects of error and timing scores on seed-based functional connectivity are summarized in Table 3.

DISCUSSION

In the current study, we demonstrate that females at increased genetic risk of developing AD exhibit significantly reduced resting-state functional connectivity within the DMN. Importantly, we observe significant correlations between DMN functional connectivity and kinematic measures of cognitive-motor performance in this group, despite no cognitive or basic motor impairment. We previously found that individuals at increased AD risk performed significantly worse on visuomotor tasks under cognitively demanding conditions [26], and that this poor performance was associated with lower WM integrity in the brain [32]. Here we extend these findings by demonstrating that poorer cognitive-motor performance in high AD-risk participants is also associated with reduced resting-state functional connectivity, including parietal-frontal, interhemispheric, and temporal-subcortical connections. These data support the power of using simple behavioral

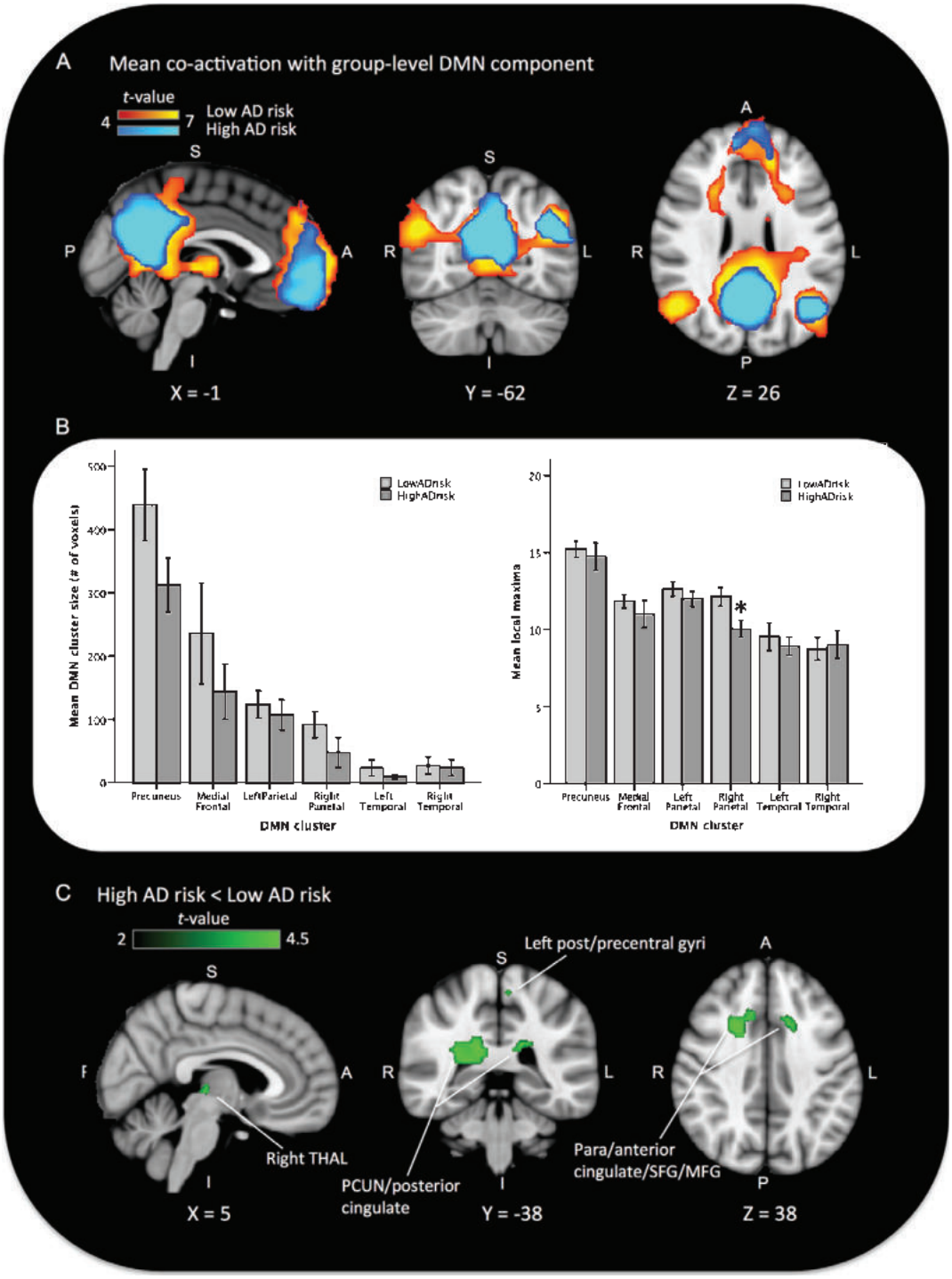

Fig. 3. A) Mean FSL MELODIC independent component analysis (ICA) activations for the default mode network (DMN) in the low (red-yellow/background) and high (blue-light blue/foreground) AD risk groups ($p < 0.02$, corrected). B) Bar graphs comparing mean (± SEM) DMN cluster sizes and peak activations (local maxima) between the low (light grey) and high (dark gray) AD risk groups. Asterisk denotes significantly lower peak activation in the right parietal cluster for the high relative to low AD risk group ($p < 0.05$). C) Regions of the DMN ICA spatial map showing significantly lower activation in high relative to low AD risk older adult participants. Group differences calculated using permutation testing (FSL randomise) and displayed at $p < 0.02$ (corrected). AD, Alzheimer's disease; S, superior; P, posterior; I, inferior; A, anterior; R, right; L, left; THAL, thalamus; PCUN, precuneus; SFG, superior frontal gyrus; MFG, middle frontal gyrus.

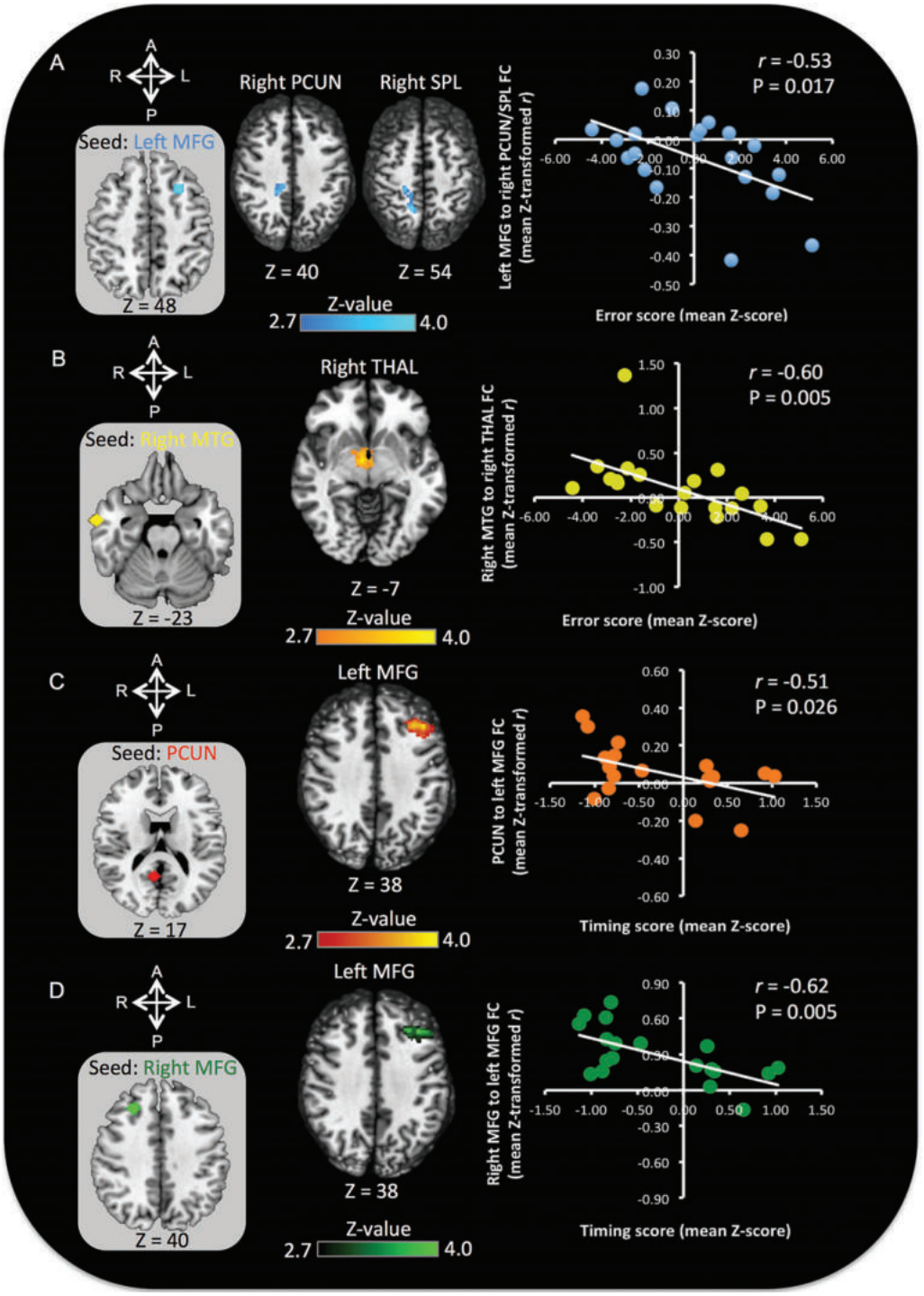

Fig. 4. *Left panel*: clusters showing significantly lower functional connectivity with (A) the left middle frontal gyrus (MFG), (B) the right middle temporal gyrus (MTG), (C) the precuneus (PCUN), and (D) the right middle frontal gyrus (MFG) in older adult participants with poorer performance (i.e., either larger error or timing scores) on a cognitively demanding visuomotor task. *Right panel*: scatterplots illustrating the significant negative correlation found between (A) left MFG to right parietal functional connectivity and performance error scores, (B) right MTG to thalamus/putamen functional connectivity and performance error scores, (C) PCUN to left MFG functional connectivity and performance timing scores, and (D) right MFG to left MFG functional connectivity and performance timing scores. R, right; L, left; A, anterior; P, posterior; SPL, superior parietal lobule; THAL, thalamus; FC, functional connectivity.

Table 2
Regions of the DMN spatial map showing significantly lower resting-state activation in high AD risk relative low AD risk older adults

Brain region	Local maxima (MNI152)				
Harvard-Oxford structural label	x	y	z	*t*-value	*p*-value
Left para/anterior cingulate/SFG	–18	18	32	4.96	0.008
Right para/anterior cingulate/MFG/SFG	22	10	36	5.08	0.008
Right PCUN/posterior cingulate	30	–50	20	5.48	0.008
Left PCUN/posterior cingulate	–18	–46	20	4.66	0.008
Right frontal pole	26	43	17	5.11	0.039
Right THAL	6	–22	0	4.33	0.008
Left post/precentral gyri	–6	–38	60	4.44	0.010

DMN, default mode network; AD, Alzheimer's disease; MNI, Montreal Neurological Institute; SFG, superior frontal gyrus; MFG, middle frontal gyrus; PCUN, precuneus; THAL, thalamus.

Table 3
Significant effects of cognitive-motor error and timing scores on functional connectivity with DMN seed regions

Seed region	Functionally connected cluster (Harvard-Oxford structural atlas)	# of voxels	x	y	z	*z*-value	*p*-value
Error score							
Left MFG	Right PCUN/LOC/SPL	324	14	–58	54	4.01	0.024
	Right postcentral gyrus/SPL		16	–44	58	3.82	
	Right post/precentral gyri		22	–34	52	3.49	
	Right posterior cingulate/PCUN		12	–32	36	3.44	
Right MTG	Right thalamus	275	6	–6	–6	3.82	0.048
	Right Pallidum/Putamen		14	2	–10	3.26	
Timing score							
PCUN	Left MFG/IFG/frontal pole	556	–42	30	36	3.85	0.0009
	Left SFG/frontal pole/MFG		–22	34	48	3.5	
Right MFG	Left MFG/frontal pole	422	–38	32	36	4.06	0.005
	Left MFG/SFG		–28	28	52	3.02	

LOC, lateral occipital cortex; SPL, superior parietal lobule; MTG, middle temporal gyrus; IFG, inferior frontal gyrus. See Table 2 for other abbreviation definitions.

tasks that require communication across brain regions processing different domains (in this case, cognition and action) to detect impairment in a clinically feasible way.

These findings are consistent with several studies demonstrating reduced functional connectivity in the DMN in preclinical AD [17–21, 46]. For example, Hedden and colleagues [17] used Aβ imaging in combination with measures of resting-state functional connectivity in the DMN to compare participants with and without high amyloid burden. After controlling for age, cognitively normal participants with high amyloid burden were shown to exhibit significantly reduced functional connectivity within numerous brain regions of the DMN, and diminished functional correlations between the hippocampus and posterior cingulate, relative to individuals with low amyloid burden. These results suggest that such disruptions, as observed in the present study, may predict the presence of Aβ in AD-affected brain regions before clinical symptoms emerge.

More recently, Sheline et al. [20] and Mormino et al. [18] have also demonstrated differences in functional connectivity associated with Aβ, including decreases between the precuneus and the left hippocampus, parahippocampus, anterior cingulate, gyrus rectus, dorsal cingulate, and superior precuneus in both AD patients and participants with high Aβ deposition. A follow-up study comparing resting-state functional connectivity in Aβ negative participants either with or without an ApoE4 allele [21] found that Aβ negative ApoE4 carriers showed similar decreased functional connectivity between the precuneus and various DMN brain regions. These results indicate that alterations in functional connectivity in genetically predisposed participants may reflect early manifestation of a genetic effect that actually precedes pathological Aβ neurotoxicity.

Notably, the current study documents the impact of early alterations in resting-state functional connectivity on behavior in preclinical AD, going beyond purely neuroimaging work. While the preclinical definition implies no decline on standardized tests of cognitive function, novel clinical assessments that can detect subtle behavioral alterations (e.g., in the kinematics of eye and limb movements) may be

useful in identifying individuals at increased AD risk [26], [27, 31, 47]. Our current and previous [32] findings support a relationship between deficits in cognitive-motor performance and alterations in structural and functional connectivity in preclinical AD. The correlations observed between parietal-frontal functional connectivity and cognitive-motor performance are consistent with the important role of reciprocal cortical networks involving parietal, temporal, and frontal regions in transforming visual-spatial and contextual information into the intrinsic joint and muscle representation required to successfully generate a goal-directed action [48–50]. Furthermore, the reduced temporal-subcortical functional connectivity observed in correlation with poorer cognitive-motor performance is consistent with the role of temporal-thalamic connections in arousal and information integration [51], as well as the role of the basal ganglia in the anticipation and selection of body movements, cognitive-motor interactions [52, 53], and multisensory integration [54].

In summary, we present novel evidence linking a clinically simple cognitive-motor integration task with underlying AD-related alterations in the default mode network. While the generalizability of this preliminary evidence is limited by the relatively small female sample and further investigation for comparison with male participants at increased AD risk is warranted (and underway by our group), this study lays the groundwork for more hypothesis-driven investigations into task-specific functional networks that may be affected in the very early stages of AD. Based on our findings, we suggest that the use of kinematic measures reflecting cognitive-motor integration holds great promise as a tool to distinguish between healthy versus pathological aging.

ACKNOWLEDGMENTS

The authors would like to thank Joy Williams for her technical expertise in the neuroimaging laboratory at York University and Heather McGregor for her assistance with the resting-state fMRI data analysis.

This work was supported by a Canadian Institutes of Health Research operating grant (MOP-125915 to L.E.S.), and a Canadian Institutes of Health Research Banting and Best Canadian Graduate Scholarship, Institute of Aging Special Recognition Award, and Ontario Women's Health Scholars Award to K.M.H.

Authors' disclosures available online (http://j-alz.com/manuscript-disclosures/15-1137r2).

REFERENCES

[1] Ewers M, Sperling RA, Klunk WE, Weiner MW, Hampel H (2011) Neuroimaging markers for the prediction and early diagnosis of Alzheimer's disease dementia. *Trends Neurosci* **34**, 430-442.

[2] Liu CC, Kanekiyo T, Xu H, Bu G (2013) Apolipoprotein E and Alzheimer disease: Risk, mechanisms and therapy. *Nat Rev* **9**, 106-118.

[3] Fratiglioni L, Ahlbom A, Viitanen M, Winblad B (1993) Risk factors for late-onset Alzheimer's disease: A population-based, case-control study. *Ann Neurol* **33**, 258-266.

[4] Green RC, Cupples LA, Go R, Benke KS, Edeki T, Griffith PA, Williams M, Hipps Y, Graff-Radford N, Bachman D, Farrer LA, MIRAGE Study Group (2002) Risk of dementia among white and African American relatives of patients with Alzheimer disease. *JAMA* **287**, 329-336.

[5] Mayeux R, Sano M, Chen J, Tatemichi T, Stern Y (1991) Risk of dementia in first-degree relatives of patients with Alzheimer's disease and related disorders. *Arch Neurol* **48**, 269-273.

[6] Storandt M, Mintun MA, Head D, Morris JC (2009) Cognitive decline and brain volume loss as signatures of cerebral amyloid-beta peptide deposition identified with Pittsburgh compound B: Cognitive decline associated with Abeta deposition. *Arch Neurol* **66**, 1476-1481.

[7] Mitchell J, Arnold R, Dawson K, Nestor PJ, Hodges JR (2009) Outcome in subgroups of mild cognitive impairment (MCI) is highly predictable using a simple algorithm. *J Neurol* **256**, 1500-1509.

[8] Agosta F, Pievani M, Geroldi C, Copetti M, Frisoni GB, Filippi M (2012) Resting state fMRI in Alzheimer's disease: Beyond the default mode network. *Neurobiol Aging* **33**, 1564-1578.

[9] Liu Y, Yu C, Zhang X, Liu J, Duan Y, Alexander-Bloch AF, Liu B, Jiang T, Bullmore E (2014) Impaired long distance functional connectivity and weighted network architecture in Alzheimer's disease. *Cereb Cortex* **24**, 1422-1435.

[10] Bartzokis G, Sultzer D, Lu PH, Nuechterlein KH, Mintz J, Cummings JL (2004) Heterogeneous age-related breakdown of white matter structural integrity: Implications for cortical "disconnection" in aging and Alzheimer's disease. *Neurobiol Aging* **25**, 843-851.

[11] Bartzokis G (2004) Age-related myelin breakdown: A developmental model of cognitive decline and Alzheimer's disease. *Neurobiol Aging* **25**, 5-18.

[12] Gold BT, Powell DK, Andersen AH, Smith CD (2010) Alterations in multiple measures of white matter integrity in normal women at high risk for Alzheimer's disease. *Neuroimage* **52**, 1487-1494.

[13] Persson J, Lind J, Larsson A, Ingvar M, Cruts M, Van Broeckhoven C, Adolfsson R, Nilsson LG, Nyberg L (2006) Altered brain white matter integrity in healthy carriers of the APOE epsilon4 allele: A risk for AD? *Neurology* **66**, 1029-1033.

[14] Reisberg B, Franssen EH, Souren LE, Auer SR, Akram I, Kenowsky S (2002) Evidence and mechanisms of retrogenesis in Alzheimer's and other dementias: Management and treatment import. *Am J Alzheimers Dis Other Demen* **17**, 202-212.

[15] Smith CD, Chebrolu H, Andersen AH, Powell DA, Lovell MA, Xiong S, Gold BT (2010) White matter diffusion alterations in normal women at risk of Alzheimer's disease. *Neurobiol Aging* **31**, 1122-1131.

[16] Bonni S, Lupo F, Lo Gerfo E, Martorana A, Perri R, Caltagirone C, Koch G (2013) Altered parietal-motor connections in Alzheimer's disease patients. *J Alzheimers Dis* **33**, 525-533.

[17] Hedden T, Van Dijk KR, Becker JA, Mehta A, Sperling RA, Johnson KA, Buckner RL (2009) Disruption of functional connectivity in clinically normal older adults harboring amyloid burden. *J Neurosci* **29**, 12686-12694.

[18] Mormino EC, Smiljic A, Hayenga AO, Onami SH, Greicius MD, Rabinovici GD, Janabi M, Baker SL, Yen IV, Madison CM, Miller BL, Jagust WJ (2011) Relationships between beta-amyloid and functional connectivity in different components of the default mode network in aging. *Cereb Cortex* **21**, 2399-2407.

[19] Petrella JR, Sheldon FC, Prince SE, Calhoun VD, Doraiswamy PM (2011) Default mode network connectivity in stable vs progressive mild cognitive impairment. *Neurology* **76**, 511-517.

[20] Sheline YI, Raichle ME, Snyder AZ, Morris JC, Head D, Wang S, Mintun MA (2010) Amyloid plaques disrupt resting state default mode network connectivity in cognitively normal elderly. *Biol Psychiatry* **67**, 584-587.

[21] Sheline YI, Morris JC, Snyder AZ, Price JL, Yan Z, D'Angelo G, Liu C, Dixit S, Benzinger T, Fagan A, Goate A, Mintun MA (2010) APOE4 allele disrupts resting state fMRI connectivity in the absence of amyloid plaques or decreased CSF Abeta42. *J Neurosci* **30**, 17035-17040.

[22] Sorg C, Riedl V, Muhlau M, Calhoun VD, Eichele T, Laer L, Drzezga A, Forstl H, Kurz A, Zimmer C, Wohlschlager AM (2007) Selective changes of resting-state networks in individuals at risk for Alzheimer's disease. *Proc Natl Acad Sci U S A* **104**, 18760-18765.

[23] de Boer C, Mattace-Raso F, van der Steen J, Pel JJ (2013) Mini-Mental State Examination subscores indicate visuomotor deficits in Alzheimer's disease patients: A cross-sectional study in a Dutch population. *Geriatr Gerontol Int* **14**, 880-885.

[24] Ghilardi MF, Alberoni M, Marelli S, Rossi M, Franceschi M, Ghez C, Fazio F (1999) Impaired movement control in Alzheimer's disease. *Neurosci Lett* **260**, 45-48.

[25] Ghilardi MF, Alberoni M, Rossi M, Franceschi M, Mariani C, Fazio F (2000) Visual feedback has differential effects on reaching movements in Parkinson's and Alzheimer's disease. *Brain Res* **876**, 112-123.

[26] Hawkins KM, Sergio LE (2014) Visuomotor impairments in older adults at increased Alzheimer's disease risk. *J Alzheimers Dis* **42**, 607-621.

[27] Salek Y, Anderson ND, Sergio L (2011) Mild cognitive impairment is associated with impaired visual-motor planning when visual stimuli and actions are incongruent. *Eur Neurol* **66**, 283-293.

[28] Tippett WJ, Sergio LE (2006) Visuomotor integration is impaired in early stage Alzheimer's disease. *Brain Res* **1102**, 92-102.

[29] Tippett WJ, Krajewski A, Sergio LE (2007) Visuomotor integration is compromised in Alzheimer's disease patients reaching for remembered targets. *Eur Neurol* **58**, 1-11.

[30] Tippett WJ, Sergio LE, Black SE (2012) Compromised visually guided motor control in individuals with Alzheimer's disease: Can reliable distinctions be observed? *J Clin Neurosci* **19**, 655-660.

[31] Verheij S, Muilwijk D, Pel JJ, van der Cammen TJ, Mattace-Raso FU, van der Steen J (2012) Visuomotor impairment in early-stage Alzheimer's disease: Changes in relative timing of eye and hand movements. *J Alzheimers Dis* **30**, 131-143.

[32] Hawkins KM, Goyal AI, Sergio LE (2015) Diffusion tensor imaging correlates of cognitive-motor decline in normal aging and increased Alzheimer's disease risk. *J Alzheimers Dis* **44**, 867-878.

[33] Carter CL, Resnick EM, Mallampalli M, Kalbarczyk A (2012) Sex and gender differences in Alzheimer's disease: Recommendations for future research. *J Womens Health* **21**, 1018-1023.

[34] Schmidt R, Kienbacher E, Benke T, Dal-Bianco P, Delazer M, Ladurner G, Jellinger K, Marksteiner J, Ransmayr G, Schmidt H, Stögmann E, Friedrich J, Wehringer C (2008) Sex differences in Alzheimer's disease. *Neuropsychiatr* **22**, 1-15.

[35] Reilly SL, Ferrell RE, Sing CF (1994) The gender-specific apolipoprotein E genotype influence on the distribution of plasma lipids and apolipoproteins in the population of Rochester, MN. III. Correlations and covariances. *Am J Hum Genet* **55**, 1001-1018.

[36] Honea RA, Swerdlow RH, Vidoni ED, Burns JM (2011) Progressive regional atrophy in normal adults with a maternal history of Alzheimer disease. *Neurology* **76**, 822-829.

[37] Mosconi L, Brys M, Switalski R, Mistur R, Glodzik L, Pirraglia E, Tsui W, De Santi S, de Leon MJ (2007) Maternal family history of Alzheimer's disease predisposes to reduced brain glucose metabolism. *Proc Natl Acad Sci U S A* **104**, 19067-19072.

[38] Mosconi L, Glodzik L, Mistur R, McHugh P, Rich KE, Javier E, Williams S, Pirraglia E, De Santi S, Mehta PD, Zinkowski R, Blennow K, Pratico D, de Leon MJ (2010) Oxidative stress and amyloid-beta pathology in normal individuals with a maternal history of Alzheimer's. *Biol Psychiatry* **68**, 913-921.

[39] Jenkinson M, Beckmann CF, Behrens TE, Woolrich MW, Smith SM (2012) Fsl. *Neuroimage* **62**, 782-790.

[40] Filippini N, MacIntosh BJ, Hough MG, Goodwin GM, Frisoni GB, Smith SM, Matthews PM, Beckmann CF, Mackay CE (2009) Distinct patterns of brain activity in young carriers of the APOE-epsilon4 allele. *Proc Natl Acad Sci U S A* **106**, 7209-7214.

[41] Jenkinson M, Bannister P, Brady M, Smith S (2002) Improved optimization for the robust and accurate linear registration and motion correction of brain images. *Neuroimage* **17**, 825-841.

[42] Smith SM (2002) Fast robust automated brain extraction. *Hum Brain Mapp* **17**, 143-155.

[43] Biswal B, Yetkin FZ, Haughton VM, Hyde JS (1995) Functional connectivity in the motor cortex of resting human brain using echo-planar MRI. *Magn Reson Med* **34**, 537-541.

[44] Zhang Y, Brady M, Smith S (2001) Segmentation of brain MR images through a hidden Markov random field model and the expectation-maximization algorithm. *IEEE Trans Med Imaging* **20**, 45-57.

[45] Raichle ME, MacLeod AM, Snyder AZ, Powers WJ, Gusnard DA, Shulman GL (2001) A default mode of brain function. *Proc Natl Acad Sci U S A* **98**, 676-682.

[46] Drzezga A, Becker JA, Van Dijk KR, Sreenivasan A, Talukdar T, Sullivan C, Schultz AP, Sepulcre J, Putcha D, Greve D, Johnson KA, Sperling RA (2011) Neuronal dysfunction and disconnection of cortical hubs in non-demented subjects with elevated amyloid burden. *Brain* **134**, 1635-1646.

[47] Mollica MA, Navarra J, Fernández-Prieto I, Olives J, Tort A, Valech N, Coll-Padrós N, Molinuevo JL, Rami L (2015) Subtle visuomotor difficulties in preclinical Alzheimer's

disease. *J Neuropsychol*. doi: 10.1111/jnp.12079 [Epub ahead of print].

[48] Battaglia-Mayer A, Ferraina S, Mitsuda T, Marconi B, Genovesio A, Onorati P, Lacquaniti F, Caminiti R (2000) Early coding of reaching in the parietooccipital cortex. *J Neurophysiol* **83**, 2374-2391.

[49] Galati G, Committeri G, Pitzalis S, Pelle G, Patria F, Fattori P, Galletti C (2011) Intentional signals during saccadic and reaching delays in the human posterior parietal cortex. *Eur J Neurosci* **34**, 1871-1885.

[50] Hawkins KM, Sayegh P, Yan X, Crawford JD, Sergio LE (2013) Neural activity in superior parietal cortex during rule-based visual-motor transformations. *J Cogn Neurosci* **25**, 436-454.

[51] Shao Y, Wang L, Ye E, Jin X, Ni W, Yang Y, Wen B, Hu D, Yang Z (2013) Decreased thalamocortical functional connectivity after 36 hours of total sleep deprivation: Evidence from resting state FMRI. *PLoS One* **8**, e78830.

[52] Middleton FA, Strick PL (2000) Basal ganglia and cerebellar loops: Motor and cognitive circuits. *Brain Res Brain Res Rev* **31**, 236-250.

[53] Leisman G, Braun-Benjamin O, Melillo R (2014) Cognitive-motor interactions of the basal ganglia in development. *Front Syst Neurosci* **8**, 16.

[54] Reig R, Silberberg G (2014) Multisensory integration in the mouse striatum. *Neuron* **83**, 1200-1212.